

Research on In-plane Fluid-elastic Instability of Heat Transfer Tube in Steam Generator

QI, Huan-huan¹

Science and Technology on Reactor System Design Technology Laboratory
Nuclear Power Institute of China, 328 Changshun Avenue, Chengdu, China

JIANG, Nai-bin²

Science and Technology on Reactor System Design Technology Laboratory
Nuclear Power Institute of China, 328 Changshun Avenue, Chengdu, China

HUANG, Xuan³

Science and Technology on Reactor System Design Technology Laboratory
Nuclear Power Institute of China, 328 Changshun Avenue, Chengdu, China

FENG, Zhi-peng⁴

Science and Technology on Reactor System Design Technology Laboratory
Nuclear Power Institute of China, 328 Changshun Avenue, Chengdu, China

ABSTRACT

Due to a small gap between the anti-vibration bars (AVBs) and the heat transfer tubes, and according to the position of AVBs and the number of continuous failures of the in-plane support, the in-plane restraint failure analysis of AVB is divided into 13 cases. The influence of the restraint failure on the in-plane mode of the heat transfer tube under different cases is analysed. The mode damping ratio was calculated by performing a weighted average method based on the mode shape function, and then the effects of different restraints by AVBs on fluid-elastic instability of steam generator tubes are studied. The analysis results show that with the increase of the continuous failure position of the in-plane support, the first-order modal frequency in the elbow zone decreases continuously, and the mode shape appearing in the elbow zone becomes more obvious. The first-order mode in the elbow zone is not necessarily the mode in which the largest fluid-elastic instability ratio occurs. The vibration mode with the largest ratio of the fluid-elastic instability appears almost in the elbow zone. With the increase of the continuous failure position of the in-plane support, the fluid-elastic instability ratio increases continuously. When three or more continuous AVBs fail in-plane, fluid-elastic instability will occur.

Keywords: Steam Generator Tube, AVBs, Fluid-elastic Instability

I-INCE Classification of Subject Number: 49

¹ qihuan73@126.com ² jnb1980@163.com

³ fengzhipengchn@163.com ⁴ 19380377@qq.com

1. INTRODUCTION

In PWR nuclear power plants, one of the main causes of unplanned shutdowns and loss of capacity factor of the plant is related to the failure of the steam generator. The steam generator heat transfer tube accounts for 80% of the total pressure boundary. In order to improve the heat transfer efficiency, the wall thickness is very thin, which is easy to cause mechanical damage and corrosion. The problem is more serious due to the high temperature of the metal.

Fluid-elastic instability is the most serious flow-induced vibration mechanism, which can cause the heat transfer tube to wear through in a short time. The steam generator design stage must ensure that the equivalent lateral flow velocity is less than the critical flow velocity when instability occurs. The elbow zone of the heat transfer tube has both in-plane and out-of-plane vibration modes, and the natural frequency of the external vibration below the same constraint is lower than the natural frequency of the in-plane vibration^[1]. The out-of-plane vibration direction is perpendicular to the flow direction, and the in-plane vibration is parallel to the flow direction (the downstream direction). Some scholars believe that the fluid-elastic instability perpendicular to the flow direction occurs before the downstream direction^[2-3]. Therefore, in the past, the nuclear industry paid more attention to the fluid-induced vibration in the out-of-plane direction of the steam generator, and often ignored the in-plane direction. AVB assembly is installed in the elbow zone of the pressurized water reactor steam generator to provide support for the elbow zone. Since the gap between AVB and the heat transfer tube is small, an effective support for the out-of-plane vibration can be ensured. Different from the mechanism of the out-of-plane direction, the in-plane support mechanism is realized by frictional constraints, and it is difficult to ensure that all in-plane constraints are effective due to the existence of the gap^[4-6]. In 2012, the SONGS nuclear power plant in the United States caused excessive fluid-induced vibration due to the heat transfer tube of the steam generator, causing some of the heat transfer tubes to be worn through, and the nuclear power plant declared permanent shutdown, causing incalculable economic losses and serious social impact. The most fundamental reason is that under the local extreme thermal hydraulic condition, the contact force of AVB on the heat transfer tube is insufficient, and the fluid-elastic instability and random vibration in the in-plane direction of the heat transfer tube cannot be effectively avoided, thereby causing wear.

In this paper, the in-plane fluid-elastic instability of steam generators is studied. The influence of the restraint failure on the in-plane mode of the heat transfer tube under different cases is analysed. The mode damping ratio was calculated by performing a weighted average method based on the mode shape function. The integrated frequency, mode shape, damping, the flow field and other factors, the effects of different restraints by AVBs on fluid-elastic instability of steam generator tubes are studied.

2. TWO PHASE FLUID-ELASTIC INSTABILITY CALCULATION METHOD

Self-excited vibration occurs when the energy dissipated by the heat transfer tube is less than the energy absorbed from the surrounding flow field. The energy absorbed by the heat transfer tube from the flow increases with the increase of the flow velocity. When the flow velocity reaches the critical value, the absorbed energy will be greater than the consumed energy. The continuous increase of energy will cause dynamic instability, the reaction increases sharply. The fluid-elastic instability is the result of strong coupling between structure and flow.

The formula for calculating the critical flow velocity of the tube under the action of lateral flow is:

$$U_c^i = \beta f_i D \left(\frac{m_0 \delta_i}{\rho_0 D^2} \right)^{0.5} \quad \text{Equation 1}$$

Where f_i is the i -th modal frequency, D is the outer diameter of tube, m_0 is the reference mass per unit length of the tube, δ_i is the damping coefficient of the i -th mode, ρ_0 the flow reference density of the secondary side, β is the instability coefficient which is related to flow field and the arrangement of the tube bundles and generally determined by experimental fitting, the recommended values are given in various literatures and ASME specifications, and the range of values is generally between 2.4 and 10.

Damping coefficient $\delta_i = 2\pi\zeta_i$, where ζ_i is damping ratio of the i -th mode, consists of the support damping ratio, the viscous damping ratio and the two-phase damping ratio. The damping ratio is greatly affected by the void fraction. According to Equation 1, in the calculation of the critical flow velocity, the damping ratio of each mode is needed to calculate, and the formula is:

$$\zeta_i = \frac{\sum_{j=1}^M \zeta_i(j) \psi_i^2(j) \Delta Z(j)}{\sum_{j=1}^M \psi_i^2(j) \Delta Z(j)} \quad \text{Equation 2}$$

Where $\zeta_i(j)$ is the damping ratio of the i -th mode at the node j , $\Delta Z(j)$ is the unit length of the node j . According to the ASME code, for multi-span heat transfer tubes with oversized tube holes supported, the damping ratio ranges from $0.008 \leq \zeta_i \leq 0.03$ when the medium is low-density gas. For the case where the void fraction is greater than 95%, the lower limit of the damping ratio of some engineering items is 0.0012.

In actual engineering, the flow field distribution in the tube bundle is non-uniform. Due to the phase transition, the difference of the void fractions in different regions is large, and the difference in flow density on the secondary side is large, which causes a large difference in the additional mass of different positions of the heat transfer tubes. Connors proposes a method for calculating the equivalent flow velocity, namely:

$$U_e^i = \left[\frac{\sum_{j=1}^M \frac{\rho(j)}{\rho_0} U^2(j) \psi_i^2(j) \Delta Z(j)}{\sum_{j=1}^M \frac{m(j)}{m_0} \psi_i^2(j) \Delta Z(j)} \right]^{0.5} \quad \text{Equation 3}$$

Where $\rho(j)$ is the secondary side flow density at the node j position, $U(j)$ is the flow velocity at the node j position, $m(j)$ is the equivalent mass of the tube unit length at the node j position.

The instability ratio is an important parameter to characterize the fluid-elastic instability. Its expression is U_e^i / U_c^i . If $U_e^i / U_c^i < 1$, no instability will occur, then $U_e^i / U_c^i \geq 1$, there is a danger of instability.

Connors' calculation method has been approved by Paidoussis, Au-Yang, etc., and is used in the design of steam generator heat transfer tubes and shell-and-tube heat exchangers.

The position where the flow velocity of the secondary side is the largest and the position where the amplitude of the low-order frequency is the largest does not necessarily coincide, so the maximum value in the equivalent flow velocity does not necessarily correspond to the first-order or low-order mode. As a result, the maximum value of the fluid-elastic instability ratio does not necessarily appear in the first-order or

low-order mode. In the engineering calculation, it is necessary to calculate the fluid-elastic instability ratio of the first few tens orders, and take the maximum value to measure the fluid-elastic instability performance of the heat transfer tube.

3. IN-PLANE MODAL CALCULATION OF TYPICAL TUBE

Select a typical heat transfer tube to create a finite element model, as shown in Figure 1. Only consider its in-plane degrees of freedom. The bottom of the heat transfer tube is fixedly supported by the tube sheet to restrain its translational and rotational freedom. There are a total of 10 plate supports along the straight pipe zone of the heat transfer tube, and the position of the support plate only constrains the horizontal translational freedom of the heat transfer tube. The elbow zone of the heat transfer tube is uniformly supported by AVBs at 12 positions. In the general engineering calculation, AVB constrains the translational freedom of the heat transfer tube. Taking into account the gap between the heat transfer tube and AVB, and considering the sharp decrease in damping under the high cavitation fraction, in the in-plane direction, AVB may fail to restrain the heat transfer tube.

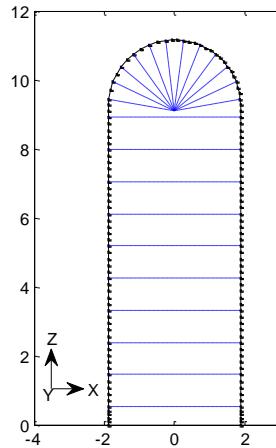


Figure 1 Finite element model of heat transfer tube

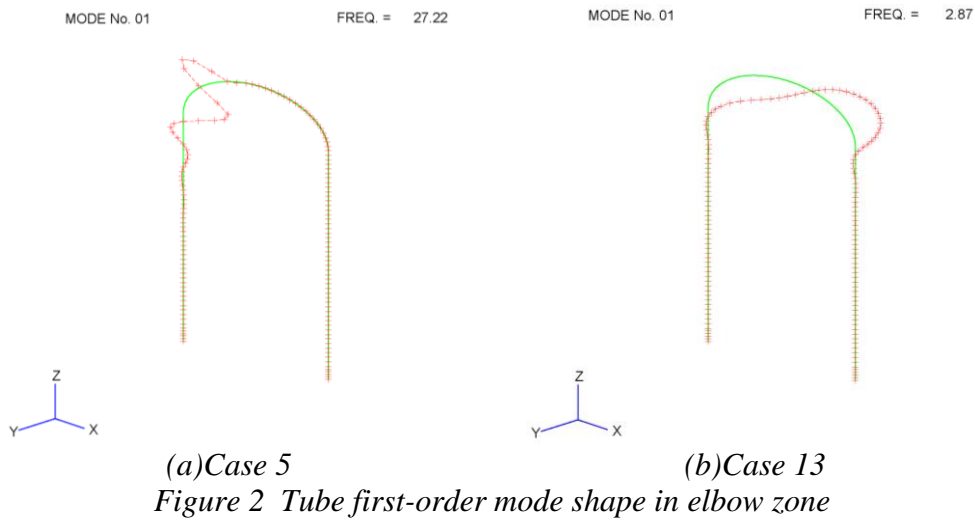
The node numbers corresponding to the 12 constraint positions of the elbow zone of the heat transfer tube are shown in Table 1. A total of 13 cases were considered, i.e. all in-plane support is effective, one in-plane support failure, two in-plane support failures... and 12 in-plane support failures.

Table 1 Analysis cases

Case	Number of in-plane support failure	Node number corresponding to the failed support
1	None	None
2	1	54
3	2	54, 56
4	3	54, 56, 58
5	4	54, 56, 58, 60
6	5	54, 56, 58, 60, 62
7	6	54, 56, 58, 60, 62, 64
8	7	54, 56, 58, 60, 62, 64, 67
9	8	54, 56, 58, 60, 62, 64, 67, 70
10	9	54, 56, 58, 60, 62, 64, 67, 70, 73
11	10	54, 56, 58, 60, 62, 64, 67, 70, 73, 76

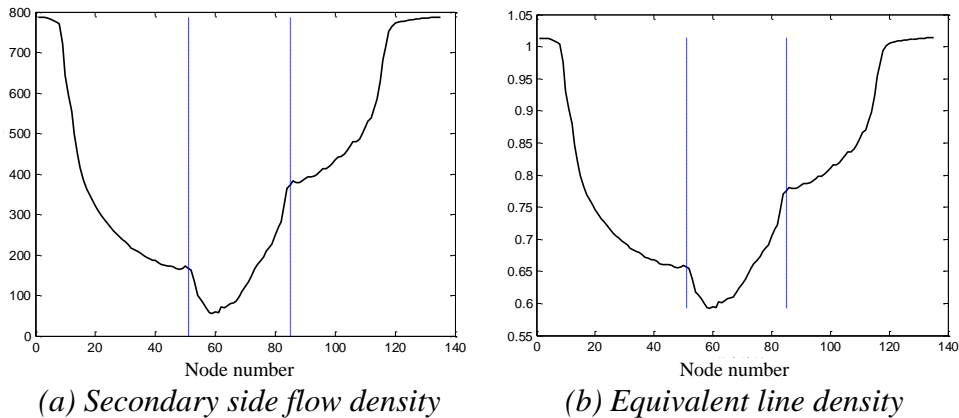
12	11	54、56、58、60、62、64、67、70、73、76、79
13	12	54、56、58、60、62、64、67、70、73、76、79、82

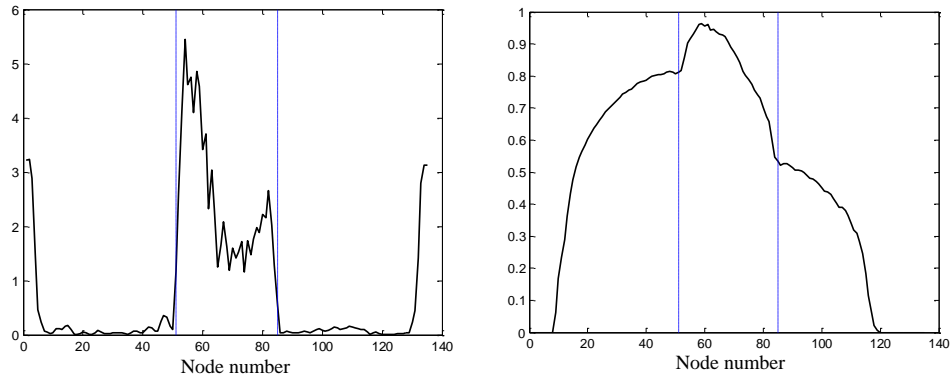
The modal analysis of 13 cases of heat transfer tubes was carried out by finite element program. The first-order natural frequency of the elbow zone is shown in Table 2. The first-order modes of the elbow zone of case 5 and case 13 are shown in Figure 2. As the in-plane support failure position increases, the first-order modal frequency in the elbow zone decreases continuously, and the amplitude appearing in the elbow zone increases. It can be seen from Figure 2 that the vibration mode basically appears in elbow zone, and the amplitude of the entire elbow zone is relatively obvious.



4. ANALYSIS OF FLUID-ELASTIC INSTABILITY

A thermal hydraulic model of the secondary side flow field was established, and the flow density, equivalent linear density, lateral flow velocity and void fraction of the secondary side of each position of the heat transfer tube were calculated, as shown in Figure 3. The equivalent density of the heat transfer tube is calculated by the secondary side flow density, and the tube cross-sectional area is multiplied to obtain the equivalent line density.





(c) Transverse flow velocity

(d) Void fraction

Figure 3 Flow parameters along tube

Through the calculation, the fluid-elastic instability ratio of the 13 cases of heat transfer tubes is obtained. Table 2 lists the frequencies under different cases, where the underlined part is the first-order in-plane modal frequency of the heat transfer tube elbow zone, and the black italic part is the modal frequency with the highest instability ratio of heat transfer tube. It can be seen from Table 2 that for case 1, the 24th order mode is the first-order mode of the elbow zone, and the maximum fluid-elastic instability ratio appears in the 47th order mode. For case 2, the 16th order mode is the first-order mode of the elbow zone, and the maximum fluid-elastic instability ratio appears in the 23rd-order mode. For case 3, the 14th order mode is the first-order mode of the elbow zone, and the maximum fluid-elastic instability ratio appears in the 24th-order mode. For case 4 - case 13, the first mode of the elbow zone is the mode in which the maximum fluid-elastic instability ratio occurs.

Table 2 Frequency under various analysis cases

Case	Frequency/Hz							
	No. 1	No. 3	No. 14	No. 16	No. 23	No. 24	No. 47	No. 48
1	37.5	41.7	75	82.1	161	<u>166</u>	<i>317</i>	324
2	37.5	41.7	72.7	<i>78.4</i>	<i>155</i>	161	311	318
3	37.5	41.7	<u>71.9</u>	78.4	154	<i>154</i>	310	311
4	37.5	<u>40.3</u>	71.6	77.3	150	154	310	311
5	<u>27.2</u>	39.6	68.4	74.8	141	147	245	280
6	<u>18.9</u>	37.6	66.2	71.6	107	141	240	245
7	<u>13.7</u>	37.5	65.3	71.6	90	111	240	241
8	<u>10.1</u>	37.5	62.3	68.4	87	90.6	227	234
9	<u>7.7</u>	29.9	60	65.6	86.4	88.3	222	227
10	<u>6</u>	24	58.3	65.3	85.4	87.5	216	221
11	<u>4.7</u>	19.6	58.2	62.3	82.9	85.4	215	216
12	<u>3.7</u>	16	54.1	60	80.5	83.6	212	215
13	<u>2.9</u>	13.2	52.9	58.5	78.3	81.6	207	213

For case 1- case 3, the amplitude of the first-order mode of the elbow zone appears less in the elbow zone, and more components appear in the straight pipe zone. Figure 4 are the mode shapes corresponding to the maximum fluid-elastic instability ratio of the heat transfer tubes of case 1 and case 3.

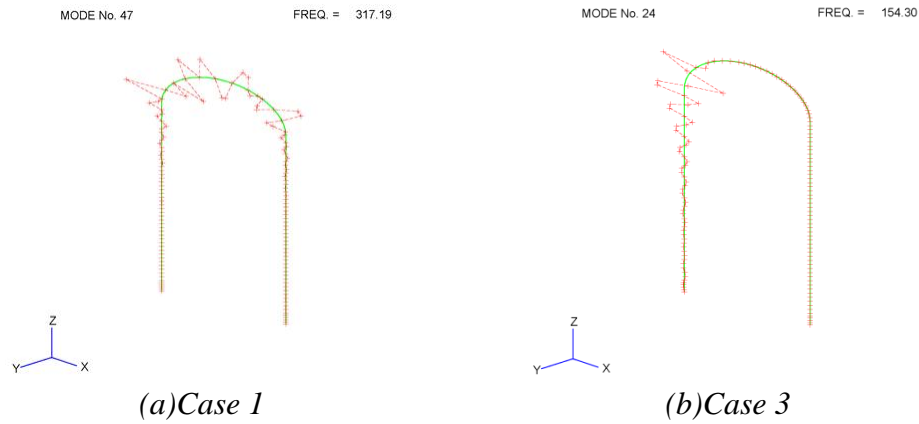


Figure 4 Mode shape corresponding to maximum ratio of fluid-elastic stability

It can be seen from Figure 4 that the mode shape with the maximum fluid-elastic instability ratio appears almost in the elbow zone. It can be seen from Figure 3 that the lateral flow velocity of the elbow zone is significantly larger than that of the straight pipe zone. The equivalent flow velocity of each mode is obtained by weighted averaging on the mode shape according to the flow velocity of each position (see Equation 3), resulting in higher equivalent flow velocities of these modes. At the same time, the damping ratio used in the critical flow velocity calculation is directly related to the void fraction. From Figure 3, it can be seen that the void fraction in the elbow zone is large, and the damping ratio is obtained by weighted averaging on the mode shape of the void fraction at each position (see Equation 2), resulting in a relatively small damping of these modes, so the critical flow velocity is low (see Equation 1). The higher equivalent flow velocity and lower critical flow velocity, the superposition of the two effects causes the fluid-elastic instability ratio of these modes to be the largest.

Table 3 lists the maximum fluid-elastic instability ratio and damping ratio for different cases. It can be seen from Table 3 that the maximum fluid-elastic instability ratio of case 1 and case 2 is the same, and the ratio increases from case 3, and the maximum fluid-elastic instability ratio is greater than 1 from case 4, indicating that fluid-elastic instability may occur. In other words, when three or more consecutive AVBs in-plane constraints fail, fluid-elastic instability may occur.

Table 3 Maximum fluid-elastic instability ratio and damping ratio for different cases

Case	Maximum fluid-elastic instability ratio	Damping ratio
1	0.40	0.002
2	0.40	0.008
3	0.59	0.005
4	1.16	0.015
5	2.54	0.01
6	3.07	0.012
7	3.57	0.015
8	4.07	0.018
9	4.55	0.022
10	5.04	0.026
11	5.64	0.03
12	6.88	0.03
13	8.58	0.03

5. CONCLUSIONS

According to the arrangement of AVB, the failure analysis of AVB in-plane constraint is divided into 13 cases. The influence of the constrained failure on the in-plane mode is analysed. The weighted average method is used to calculate the damping ratio of each mode. Then the effects of different restraints by AVBs on fluid-elastic instability of steam generator tubes are studied. The following conclusions are obtained.

(1) With the increase of the continuous failure position of the in-plane support, the first-order modal frequency in the elbow zone is continuously reduced, and the vibration mode appearing in the elbow portion becomes more obvious.

(2) The first-order mode in the elbow zone is not necessarily the mode in which the maximum instability ratio occurs. The mode shape with the maximum stray instability ratio appears almost in the elbow zone.

(3) The lateral flow velocity of the elbow zone is significantly larger than that of the straight pipe zone, resulting in a higher equivalent flow velocity of these modes; at the same time, the void fraction of the elbow zone is large, which causes the damping of these modes to be relatively small, so the critical flow velocity is low; the superposition of the two effects causes the instability ratio of these modes to be the largest.

(4) With the increase of the continuous failure position of the in-plane support, the in-plane fluid-elastic instability ratio increases continuously. When three or more consecutive AVBs in-plane constraints fail, fluid-elastic instability may occur.

In the calculation, it is assumed that AVB has continuous failure of the in-plane support of the elbow zone, which may be different from the actual situation. In actual operation, AVB may produce a pre-tightening force on the heat transfer tube, which has a certain constraint on the vibration in the in-plane direction. Therefore, the assumption of continuous in-plane constrained failure in this paper is conservative.

6. ACKNOWLEDGEMENTS

This project is supported by National Natural Science Foundation of China (Grant No. 51606180 and No. 11872060)

7. REFERENCES

1. Chu I. C., Chang H. J., Lee C. H. “*Fluid-elastic instability of rotated square array U-tube in air-water flow*”, ASME Journal of Pressure Vessel Technology, 2009, 131: 1-8.
2. Violette R., Mureithi N. W., Pettigrew M. J. “*Two-phase flow induced vibration of an array of tubes preferentially flexible in the flow direction*”, Proceedings of the ASME 2005 Pressure Vessels and Piping Conference, Colorado: ASME, 2005.
3. Mureithi N. W., Zhang C., Ruel M., et al. “*Fluidelastic instability tests on an array of tubes preferentially flexible in the flow direction*”, Journal of fluids and structure, 2005, 21: 75-87.
4. Weaver D. S., Schneider W. “*The effect of flat bar supports on the cross flow induced response of heat exchanger U-tubes*”, Journal of engineering for Power, 1983, 105: 775-781.
5. Nakamura T., Shimamura K., Iwase T., et al. “*Fluidelastic instability of a U-bend tube array based on correlated unsteady fluid force in two-phase flow*”, Proceedings of the ASME 2003 Pressure Vessels and Piping Conference, 2003.
6. Price S. J. “*An investigation on the use of Connor's equation to predict fluidelastic instability in cylinder arrays*”, ASME Journal of pressure vessel technology, 2001, 123: 448-453.